ChemComm

COMMUNICATION

Cite this: *Chem. Commun.*, 2020, **56**, 5552

Received 29th December 2019, Accepted 2nd April 2020

DOI: 10.1039/c9cc10041e

rsc.li/chemcomm

Aza-crown ether locked on polyethyleneimine: solving the contradiction between transfection efficiency and safety during *in vivo* gene delivery†

Shengran Li,‡[ab] Lin Lin,‡[c] Wenliang Wang,[d] Xinxin Yan,[ab] Binggang Chen,[ab] Sangni Jiang,[ab] Sanrong Liu,*[a] Xiaojing Ma,*[a] Huayu Tian[bc] and Xifei Yu*[ab]

We proposed a method using an aza-crown ether derivative to lock a hyperbranched polyethyleneimine, which endows the PEI_{25k} with tumor targeting ability, anti-serum ability and extended circulation in the blood meanwhile retaining the high gene complexation and high transfection efficiency. The method we proposed here simultaneously endows cationic materials with high transfection efficiency and high safety, which greatly pushed the cationic materials to be applied in *in vivo* gene delivery.

Researchers developing gene delivery vectors face a great challenge, that is, vectors with high transfection efficiency usually exhibit high cytotoxicity.[1] Cationic materials, specifically hyperbranched polyethyleneimine (PEI_{25k}), have been investigated as gene carriers because of their superior gene complexing ability and high transfection efficiency.[2] However, these cationic materials exhibit high cytotoxicity due to the lack of tumor targeting, serum resistance, and extended circulation in the blood.[3] This toxicity severely limits their *in vivo* application. Currently, polyethylene glycol (PEG) is grafted onto cationic materials to shield their binding to cell membranes, thus allowing the complex to accumulate at tumor sites.[3a,4] Although the increase in grafted PEG leads to longer blood circulation, it reduces the gene complexing ability and transfection efficiency of the cationic materials because of the reduction in the positive charge density.[5] Therefore, it is essential to determine a method to overcome these current limitations and generate gene delivery vectors with both high transfection efficiency to cancer cells and low toxicity to healthy cells.[6]

Crown ethers, cyclic organic compounds composed of several ether units, are capable of binding cations[7] and have been explored as phase transfer catalysts for metal extraction and supramolecular chemistry[8] and as fluorescence probes.[7,9] These properties inspired us to combine crown ethers with abundant amino cations in cationic materials to prevent the binding of cationic materials to cell membranes *via* steric hindrance. We altered the structure of the crown ether to aza-18-crown-6 ether (ACE) that can be detached from the cationic materials when exposed to the acidic environment of the tumor sites. Moreover, we linked GE11 (Y-H-W-Y-G-Y-T-P-Q-N-V-I), an EGFR over-expressed cancer cell-targeting peptide,[10] to the ACE to make it an active target. We chose PEI_{25k} as a primary transfection reagent due to its well-known gene complexing ability and transfection efficiency. As shown in Scheme 1, the previously prepared ACE–GE11 was mixed with the PEI_{25k}/DNA complex to obtain the final nanoparticle. The working principle of this nanoparticle is as follows: the crown ether in ACE–GE11 can be stably combined with the outermost amino cation of the PEI_{25k}/DNA complex by host–guest interactions and hydrogen bonds.[11] The amino cations locked by ACE–GE11 will neither bind to the cell membrane nor bind to proteins in the blood due to the steric hindrance surrounding the amino cations. This facilitates the nanoparticles of ACE–GE11/(PEI/DNA) to be stable and remain circulating in the blood for an extended period. The targeting peptide GE11 could lead the nanoparticles to accumulate at the tumor site. When the nanoparticles arrive at the tumor site, the tertiary amines on ACEs would partially become positively charged due to the slightly acidic environment of the tumor sites. Thereafter, ACE–GE11 would detach from PEI/DNA complex owing to charge repulsion with the amino cations on PEI_{25k}, making the nanoparticles more susceptible to endocytosis by cancer cells. After endocytosis, the tertiary amines on ACEs would be completely protonated and detach from the PEI/DNA complex while entering the lysosome. The nanoparticles of PEI/DNA were entirely exposed and showed high transfection efficiency and toxicity to kill the cancer cells. Compared with the widely used PEG or other methods, the nanoparticle prepared using the ACE derivative is smaller sized and with more functions (shielding, targeting, and detaching). It is

[a] *Laboratory of Polymer Composites Engineering, Changchun Institute of Applied Chemistry, Chinese Academy of Sciences, Changchun, Jilin 130022, China. E-mail: liusanrong@ciac.ac.cn, xjma@ciac.ac.cn, xfyu@ciac.ac.cn*

[b] *University of Science and Technology of China, Hefei, Anhui 230026, China*

[c] *Laboratory of Polymer Ecomaterials, Changchun Institute of Applied Chemistry, Chinese Academy of Sciences, Changchun, Jilin 130022, China*

[d] *Department of Neurology, Johns Hopkins University School of Medicine, Baltimore, MD 21205, USA*

† Electronic supplementary information (ESI) available: Experimental details, characterization, and *et al.* See DOI: 10.1039/c9cc10041e

‡ The authors contributed equally to this work.

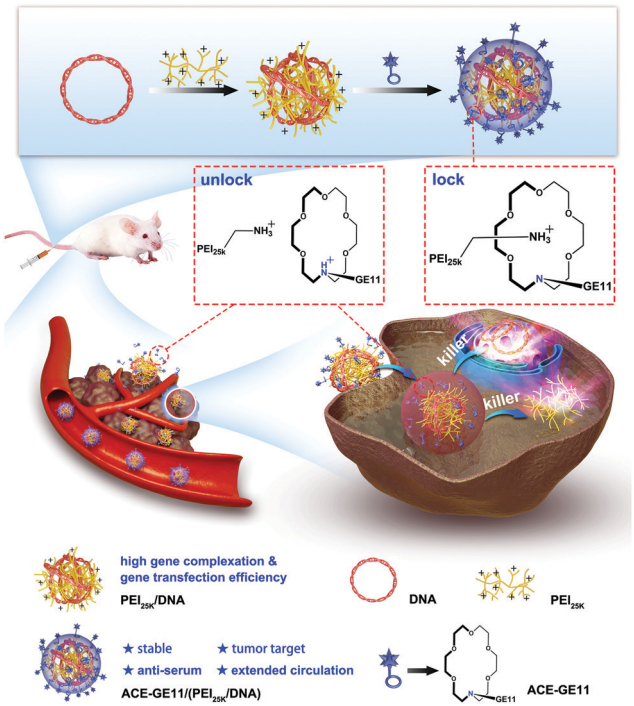

Scheme 1 Schematic of how the ACE–GE11 locks on PEI_{25k} to shield endocytosis in the blood circulation and unlocks at tumor sites.

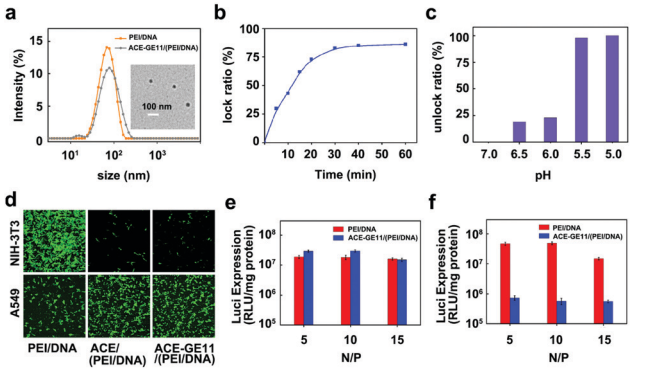

Fig. 1 (a) Size of the nanoparticles of ACE–GE11/(PEI/DNA) detected by DLS and TEM; scale bar: 100 nm. (b) The binding kinetics of ACE on PEI. Lock ratio is the molar ratio of ACE/($-NH_3^+$ on PEI). (c) The ratio of ACE unlocked from PEI_{25k} at different pH values in 2 h. (d) GFP gene transfection of the complexes of our materials and DNA at N/P = 10 on NIH-3T3 and A549 cells. Luciferase gene transfection of the complexes of our materials and DNA at different N/P ratios on (e) A549 cells and (f) NIH-3T3 cells.

more convenient to prepare (physically mixed ACE with PEI/DNA rather than chemical modification[12]) and has better shielding effects (one ACE shields one amino cation). Finally, it detaches faster in tumor sites by electrostatic repulsion rather than chemical bond rupture.[13] These properties together are more practical during gene delivery.

The product ACE–GE11 was synthesized according to the procedure described in Scheme S1 (see the ESI†) and was characterized by NMR (Fig. S1–S6, ESI†) and MALDI-TOF-MS (Fig. S7, ESI†) analysis. The complex of PEI_{25k}/DNA showed an optimal size (70 ± 2 nm) and zeta potential ($+23 \pm 3$ mV) at N/P = 10 compared with other N/Ps,[14] which were detected by dynamic light scattering (DLS) (Fig. S8 and S9, ESI†). After mixing ACE–GE11 with PEI_{25k}/DNA, the size of the nanoparticles of ACE–GE11/(PEI/DNA) was 60 nm (Fig. 1a), which was detected using an transmission electron microscope (TEM) while the zeta potential of the nanoparticles decreased to +17 mV (Fig. S9, ESI†). The changes in the size and charge indicated that ACE–GE11 was bound to PEI/DNA successfully.

To investigate the lock and unlock ability of ACE–GE11 on the amino cations of PEI_{25k}, we used ACE to mix with PEI_{25k}. The ACE/PEI complex was dialyzed with phosphate-buffered saline (PBS) to remove ACEs that were not combined to PEI_{25k}. After dialysis, the complexes of ACE/PEI were freeze-dried and ACE was eluted by CH_2Cl_2 to calculate the binding kinetics (Fig. 1b). This calculation was based on the ratio of primary, secondary, and tertiary amines on PEI_{25k}, which was 1 : 2 : 1. Only primary amines protonated in water could be combined with aza-18-crown-6 ether (ACE) by host–guest interactions and hydrogen bonds, while other amino cations on PEI could not.[11,15]

We found that 83% of $-NH_3^+$ on PEI was locked by ACE within 30 minutes, and the limit of the lock ratio was 86%. We also used NMR to monitor the binding process, and found that the lock ratio could be 82% in 30 minutes (Fig. S11, ESI†). We detected the binding affinity of ACE on PEI in NaCl solutions (Fig. S12, ESI†), and we found the lock ratio remained 83% in a 1% NaCl solution (the NaCl content in blood is 0.9%). This strong binding affinity was due to the formation of hydrogen bonds between ACE and PEI reference. We added the ACE/PEI complex to water with different pH, dialyzed to remove the free ACE and then analyzed by NMR (Fig. S13, ESI†). The results are shown in Fig. 1c. We found that 20% of ACE detached from PEI_{25k} at pH = 6.0–6.5 and 100% at pH = 5.0–5.5 in 2 h due to the protonation of the tertiary amine on ACE in an acidic environment and electrostatic repulsion from the amino cations on PEI_{25k}. This result indicated that when the nanoparticles of ACE–GE11/PEI/DNA arrive at the tumor area (pH = 6.0–6.5), ACE–GE11 would partially detach from the nanoparticles to enhance the endocytosis of the nanoparticles. After entering the lysosome, ACE–GE11 would completely detach from the nanoparticles, thus maximizing the transfection efficiency of PEI_{25k}. We also explored the detachment speed of ACE from PEI under acidic conditions and found that 44% of ACE were detached at 30 min and were almost fully detached in 1 h (Fig. S14 and S15, ESI†). This acidic-response speed was much faster than chemical bond cleavages, such as acetal bonds and hydrazone bonds.[16]

The effects of ACE–GE11 on shielding healthy cells transfection and targeting cancer cells were measured using green fluorescence protein reporter gene (pGFP). We found that PEI_{25k} showed high transfection efficiency on mouse embryo fibroblast (NIH-3T3) cells and human lung cancer (A549) cells (Fig. 1d). After PEI_{25k} was locked by ACE or ACE–GE11, their transfection efficiency decreased to a value quite low in healthy (NIH-3T3) cells, while increasing much in cancer (A549) cells. We found that the nanoparticles of ACE–GE11/(PEI/DNA) were shielded and could

not be endocytosed by NIH-3T3 cells regardless of the N/P ratio (Fig. S16, ESI†). These nanoparticles could be endocytosed by A549 cells and showed higher transfection efficiency than the nanoparticles of PEI/DNA (Fig. S17, ESI†). Furthermore, a luciferase plasmid (pGL3) was used as a reporter gene to evaluate the transfection efficiency of our materials. We found that the nanoparticles of ACE–GE11/(PEI/DNA) showed a higher transfection efficiency than PEI/DNA at all N/P ratios in the A549 cells (Fig. 1e). The transfection efficiency of ACE–GE11/(PEI/DNA) decreased at least 60 times compared with PEI/DNA in the NIH-3T3 cells due to the shield effect of ACE–GE11 (Fig. 1f).

We used fluorescence labelling of DNA (cy5-DNA) and confocal laser scanning microscopy (CLSM) to trace the transportation of genes by our nanoparticles. The results showed that the nanoparticles of ACE–GE11/(PEI/DNA) were quickly endocytosed and delivered to the nucleus in 1 h by A549 cells, whereas they were not endocytosed by the NIH-3T3 cells (Fig. 2a). The detailed time-dependent fixed CLSM studies of gene transportation by ACE–GE11/(PEI/DNA) on the NIH-3T3 cells and A549 cells are shown in Fig. S18–S20 (ESI†). The flow cytometry results showed that the luciferase expression of ACE–GE11/(PEI/DNA) was higher than PEI/DNA on the A549 cells (Fig. 2b), while ACE–GE11/(PEI/DNA) showed a decreased luciferase expression in the NIH-3T3 cells (Fig. 2c). The GFP, luci-expression, CLSM, and flow cytometry results were consistent, which indicated that ACE–GE11 could inhibit the healthy cell endocytosis of PEI/DNA while targeting cancer cells.

We added 10%, 30%, and 50% fetal bovine serum (FBS) to the A549 cells to investigate the ability of the serum resistance of our nanoparticles. ACE–GE11/(PEI/DNA) showed high luciferase expression with 10%, 30%, and 50% FBS, while PEI/DNA showed low luci-expressions with FBS (Fig. 2d). The GFP results shown in Fig. S21 (ESI†) indicated that PEI/DNA locked by ACE–GE11 could resist the medium with 30% FBS, while PEI/DNA could not resist any amount of FBS.

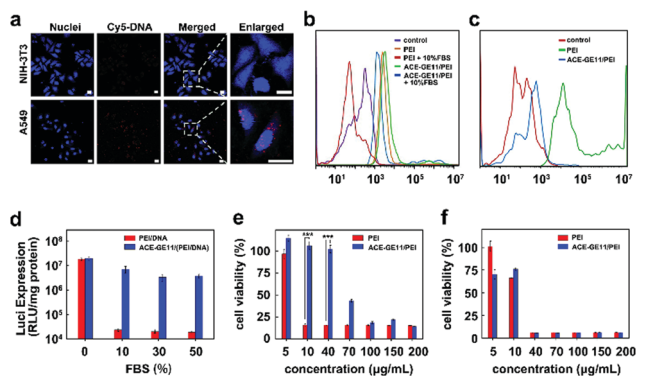

Fig. 2 (a) CLSM images of the NIH-3T3 and A549 cells cultured with ACE–GE11/(PEI_{25k}/cy5-DNA) complexes for 1 h; cy5-DNA and cell nuclei stained with DAPI are shown in red and blue, respectively; scale bars: 20 μm. GFP-positive A549 cells (b) and NIH-3T3 cells (c) measured by flow cytometry after treatment with the complexes of our materials and DNA with or without serum. (d) Luciferase gene transfection of the complexes of our materials and DNA at N/P = 10 with different amount of FBS. Cell viability of (e) NIH-3T3 cells and (f) A549 cells incubated with varying concentrations of PEI_{25k} and ACE–GE11/PEI_{25k} for 24 h; the abscissa refers to the concentration of PEI_{25k}.

To verify if ACE–GE11 could substantially improve the safety of PEI_{25k}, we evaluated the cytotoxicity of our materials by Celltiter-Blue assay. ACE–GE11 showed no toxicity to the NIH-3T3 cells, even under the concentration of 200 μg mL^{-1} (Fig. S22, ESI†). PEI_{25k} had potent cytotoxicity to the NIH-3T3 cells and A549 cells, and the cells could not survive at 10 μg mL^{-1} (Fig. 2e and f). However, after PEI_{25k} was locked by ACE–GE11, 100% of the NIH-3T3 cells survived at the concentration of 40 μg mL^{-1} of PEI_{25k} (Fig. 2e). Interestingly, ACE–GE11/PEI_{25k} showed that no A549 cancer cells survived at 40 μg mL^{-1} of PEI_{25k} (Fig. 2f). The results indicated that ACE–GE11 could significantly improve the safety of PEI_{25k} to healthy cells while maintaining substantial toxicity to cancer cells. The hemolysis test confirmed that ACE–GE11/(PEI/DNA) showed no cytotoxicity to red blood cells even at 150 μg mL^{-1}, while PEI/DNA killed red blood cells at 40 μg mL^{-1} (Fig. S23 and S24, ESI†).

The tumor accumulation of our materials was studied by tail-vein injection into an A549 xenograft mouse model, and the fluorescence images were recorded at different times (Fig. 3a). The nanoparticles of ACE–GE11/(PEI/DNA) showed substantial accumulation at 12 h after injection and continued to 24 h. The nanoparticles of PEI/DNA did not accumulate at tumor sites.

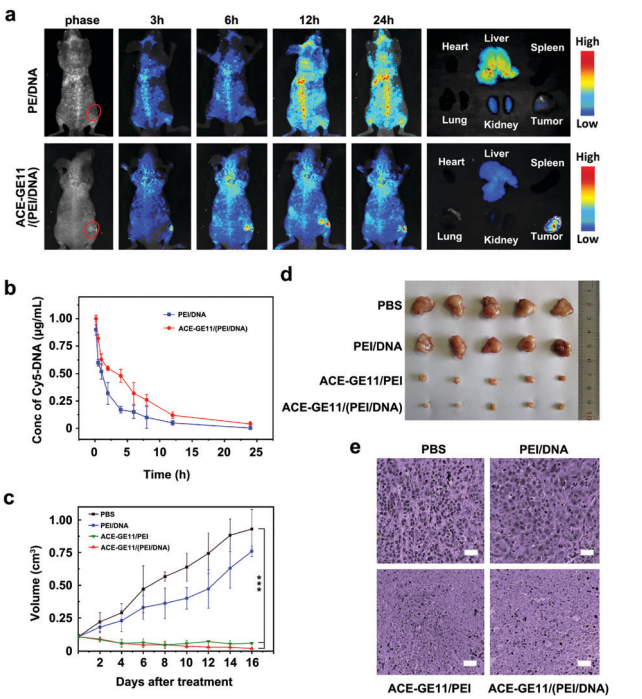

Fig. 3 (a) *In vivo* fluorescence imaging of the A549 tumor bearing mice at different times after the intravenous injection of the complexes of our materials and cy5-DNA; *Ex vivo* fluorescence imaging of various organs and tumors excised from the mice after injection for 24 h (the right). (b) The pharmacokinetics of cy5-DNA in the blood after the mice were intravenously injected with different samples. (c) Tumor growth curves in the A549 tumor bearing mice treated with different samples; DNA: caspase-3 1 mg kg^{-1}; PEI/DNA: N/P = 10; the sample ACE–GE11/PEI: PEI 3 mg kg^{-1}. (d) Representative images of the tumors *via* different treatments after 18 days. (e) H&E analysis of the tumors after 18 days of treatment *via* different reagents. Scale bars: 50 μm.

The tumor and main organs of the two groups were harvested at 24 h post-injection (Fig. 3a). Most of the nanoparticles of PEI/DNA were accumulated at the liver site, while most of the ACE–GE11/(PEI/DNA) accumulated at the tumor site and showed little accumulation in the liver. Pharmacokinetic analysis determined that ACE–GE11/(PEI/DNA) circulated longer in blood than PEI/DNA (Fig. 3b).

To investigate the antitumor efficacy of our materials, the A549 tumor-bearing mice were administered different samples intravenously. We found that the tumor growth of the mice injected with ACE–GE11/(PEI/DNA) were efficiently suppressed and the tumor size diminished. However, the mice treated with PEI/DNA had tumors that continued to increase (Fig. 3c, d and Fig. S25, ESI†). The tumor suppression ratio was calculated, as shown in Fig. S26 (ESI†), and ACE–GE11/(PEI/DNA) showed high tumor suppression up to 97.8%.[17] We also treated the mice with ACE–GE11/PEI at the dose of PEI_{25k} that was 3 mg kg^{-1} without DNA. Interestingly, we found that the tumor growth was efficiently suppressed (Fig. 3c, d and Fig. S25, ESI†), and the mice remained healthy. This result suggested that PEI_{25k} locked by ACE–GE11 was not toxic to healthy cells but highly toxic to cancer cells at a large dose of PEI_{25k}. The mice treated with ACE–GE11-locked materials were healthy and their body weights were maintained at 22–23 g, whereas the weight of the mice treated with PBS or PEI/DNA significantly decreased (Fig. S27, ESI†). Hematoxylin and eosin (H&E) assays were used to used to evaluate the antitumor efficiency of our materials. As shown in Fig. 3e, the ACE–GE11-locked materials exhibited marked necrosis of tumor cells and negligible damage to healthy organs (Fig. S28, ESI†), while PEI/DNA showed substantial toxicity to livers but low toxicity to tumors.

In conclusion, we tested a method using aza-crown ether derivatives to lock on PEI_{25k} so as to confer it with tumor targeting, anti-serum and extended blood circulation while maintaining the transfection efficiency and gene complexing ability of PEI_{25k}. Compared with the widely used modified PEG or other methods, the ACE derivative was smaller with more functionality and convenient usage by mixing it with cationic materials. Furthermore, ACE showed better shield effect in the blood and faster detachment from the complex when reaching the tumor sites. The method we proposed breaches the barrier between transfection efficiency and safety in gene carriers and shows promise for *in vivo* gene therapy.

The animal experiments were approved by the Animal Care and Use Committee of Northeast Normal University. All operations were performed according to international guidelines concerning the care and treatment of experimental animals. The case number of institutional approval of the animal is SCXK(Jing)2016-0006. Financial support from the Nation Natural Science Foundation of China (21674109) is gratefully acknowledged.

Conflicts of interest

There are no conflicts to declare.

Notes and references

1 (*a*) Z. Zhou, X. Liu, D. Zhu, Y. Wang, Z. Zhang, X. Zhou, N. Qiu, X. Chen and Y. Shen, *Adv. Drug Delivery Rev.*, 2017, **115**, 115–154; (*b*) H. Yin, R. L. Kanasty, A. A. Eltoukhy, A. J. Vegas, J. R. Dorkin and D. G. Anderson, *Nat. Rev. Genet.*, 2014, **15**, 541–555.

2 (*a*) M. S. Shim and Y. Xia, *Angew. Chem., Int. Ed.*, 2013, **52**, 6926–6929; (*b*) S. Liu, D. Zhou, J. Yang, H. Zhou, J. Chen and T. Guo, *J. Am. Chem. Soc.*, 2017, **139**, 5102–5109; (*c*) S. Kim, S. J. Yu, I. Kim, J. Choi, Y. H. Choi, S. G. Imc and N. S. Hwang, *Chem. Commun.*, 2019, **55**, 2317.

3 (*a*) H. J. Vaughan, J. J. Green and S. Y. Tzeng, *Adv. Mater.*, 2019, e1901081; (*b*) S. Li, X. Yan, Y. Qu, W. Wang, B. Chen, X. Ma, S. Liu and X. Yu, *Chem. – Eur. J.*, 2019, **25**, 1–11.

4 (*a*) W. Yasen, R. Dong, L. Zhou, Y. Huang, D. Guo, D. Chen, C. Li, A. Ainic and X. Zhu, *Chem. Commun.*, 2017, **53**, 12782; (*b*) B. Zoetebier, A. Sohrabi, B. Lou, M. A. Hempenius, W. E. Hennink and G. J. Vancso, *Chem. Commun.*, 2016, **52**, 7707.

5 (*a*) H. Hatakeyama, H. Akita and H. Harashima, *Adv. Drug Delivery Rev.*, 2011, **63**, 152–160; (*b*) W. F. Lai, *Expert Rev. Med. Devices*, 2011, **8**, 173–185.

6 C. E. Dunbar, K. A. High, J. K. Joung, D. B. Kohn, K. Ozawa and M. Sadelain, *Science*, 2018, 359.

7 J. Li, D. Yim, W. D. Jang and J. Yoon, *Chem. Soc. Rev.*, 2017, **46**, 2437–2458.

8 D. Aoki, G. Aibara, S. Uchida and T. Takata, *J. Am. Chem. Soc.*, 2017, **139**, 6791–6794.

9 M. Isik, R. Guliyev, S. Kolemen, Y. Altay, B. Senturk, T. Tekinay and E. U. Akkaya, *Org. Lett.*, 2014, **16**, 3260–3263.

10 J. Pi, J. Jiang, H. Cai, F. Yang, H. Jin, P. Yang, J. Cai and Z. W. Chen, *Drug Delivery*, 2017, **24**, 1549–1564.

11 P. R. Ashton, E. J. T. Chrystal, P. T. Glink, S. Menzer, C. Schiavo, N. Spencer, J. F. Stoddart, P. A. Tasker, A. J. P. White and D. J. Williams, *Chem. – Eur. J.*, 1996, **2**, 709–728.

12 X. Guan, Z. Guo, T. Wang, L. Lin, J. Chen, H. Tian and X. Chen, *Biomacromolecules*, 2017, **18**, 1342–1349.

13 S. Mura, J. Nicolas and P. Couvreur, *Nat. Mater.*, 2013, **12**, 991–1003.

14 Z. Chen, W. Huang, N. Zheng and Y. Bai, *Polym. Chem.*, 2020, **11**, 664.

15 G. W. Gokel, W. M. Leevy and M. E. Weber, *Chem. Rev.*, 2004, **104**, 2723–2750.

16 F. Seidi, R. Jenjob and D. Crespy, *Chem. Rev.*, 2018, **118**, 3965–4036.

17 H. Fang, J. Chen, L. Lin, F. Liu, H. Tian and X. Chen, *ACS Appl. Mater. Interfaces*, 2019, **11**, 47785–47797.